Meteorologische Zeitschrift, Vol. 25, No. 3, 251–266 (published online March 21, 2016)

Mettools IX

Surface Conductance of Five Different Crops Based on 10 Years of Eddy-Covariance Measurements

Uwe Spank*, Barbara Köstner, Uta Moderow, Thomas Grünwald and Christian Bernhofer

[1]Institute of Hydrology and Meteorology, Faculty of Environmental Sciences, Technische Universität Dresden, Tharandt, Germany

(Manuscript received August 27, 2015; in revised form December 7, 2015; accepted December 19, 2015)

Abstract

The Penman-Monteith (PM) equation is a state-of-the-art modelling approach to simulate evapotranspiration (ET) at site and local scale. However, its practical application is often restricted by the availability and quality of required parameters. One of these parameters is the canopy conductance. Long term measurements of evapotranspiration by the eddy-covariance method provide an improved data basis to determine this parameter by inverse modelling. Because this approach may also include evaporation from the soil, not only the 'actual' canopy conductance but the whole surface conductance (g_c) is addressed. Two full cycles of crop rotation with five different crop types (winter barley, winter rape seed, winter wheat, silage maize, and spring barley) have been continuously monitored for 10 years. These data form the basis for this study. As estimates of g_c are obtained on basis of measurements, we investigated the impact of measurements uncertainties on obtained values of g_c. Here, two different foci were inspected more in detail. Firstly, the effect of the energy balance closure gap (EBCG) on obtained values of g_c was analysed. Secondly, the common hydrological practice to use vegetation height (h_c) to determine the period of highest plant activity (i.e., times with maximum g_c concerning CO_2-exchange and transpiration) was critically reviewed. The results showed that h_c and g_c do only agree at the beginning of the growing season but increasingly differ during the rest of the growing season. Thus, the utilisation of h_c as a proxy to assess maximum g_c ($g_{c,\max}$) can lead to inaccurate estimates of $g_{c,\max}$ which in turn can cause serious shortcomings in simulated ET. The light use efficiency (LUE) is superior to h_c as a proxy to determine periods with maximum g_c. Based on this proxy, crop specific estimates of $g_{c,\max}$ could be determined for the first (and the second) cycle of crop rotation: winter barley, 19.2 mm s^{-1} (16.0 mm s^{-1}); winter rape seed, 12.3 mm s^{-1} (13.1 mm s^{-1}); winter wheat, 16.5 mm s^{-1} (11.2 mm s^{-1}); silage maize, 7.4 mm s^{-1} (8.5 mm s^{-1}); and spring barley, 7.0 mm s^{-1} (6.2 mm s^{-1}).

Keywords: big leaf model, canopy conductance, canopy resistance, energy balance closure, error analysis, evapotranspiration, hydrological modelling, light use efficiency, Penman-Monteith approach, site water budget, soil evaporation, transpiration, uncertainty assessment

1 Introduction

Carefully executed hydrological investigations are prerequisites for adequate water resource and land use management. Analysis and quantification of actual evapotranspiration (ET) are thereby especially important. However, correct assessment of ET rates is also challenging as ET is affected by atmospheric and landscape parameters. The quantity of ET as well as its temporal characteristic is a complex result of manifold feedbacks between meteorological drivers (i.e., precipitation, radiation, air humidity and air temperature), geo-hydrological conditions (e.g. soil, relief, geological properties) and surface characteristics such like type, physiology and structure of vegetation. Thus, sophisticated model approaches are mandatorily required for physically exact description of underlying processes and for correct assessment of ET rates (Klemeš, 1983; Vicente-Serrano and López-Moreno, 2005; Sposito, 2008).

The Penman-Monteith (PM; Penman, 1948; Monteith, 1965) approach is still the state-of-the-art approach for modelling of ET at site and local scale (Xu and Singh, 1998; McMahon et al., 2013). This physically based approach utilizes a resistance analogy. It provides a suitable tool for simulation of ET from surfaces covered by low vegetation (e.g., crops). Besides this, it is also a suited tool to analyse impacts of anthropogenic modifications on the meteorological and hydrological environment (Wang and Dickinson, 2012) as it is based on physical principals. However, the practical application of the PM approach is often restricted by availability and representativeness of required parameters. If this single layer 'big-leaf' approach is expanded to cover sparse canopies in a two-layer model (Shuttleworth and Wallace, 1985), the parameterisation becomes even more complex (Stannard, 1993; Bernhofer et al., 1996).

The scientific literature provides numerous guidelines and reference parameter sets for various plant

*Corresponding author: Uwe Spank, TU Dresden, Fakultät Umweltwissenschaften, Professur für Meteorologie, 01062 Dresden, Germany, e-mail: Uwe.Spank@tu-dresden.de

DOI 10.1127/metz/2016/0732

Gebrüder Borntraeger Science Publishers, Stuttgart, www.borntraeger-cramer.com

species and vegetation types in different climate zones. An advanced example might be the Plant Parameter Database (Breuer and Frede, 2003). Nevertheless, parameterisations of different authors are often significantly different for identical plant species even under similar climate conditions (for details see the comprehensive review of Körner, 1995). Partly, this diversity can be explained by genetic variations (Kelliher et al., 1995). However, different site conditions (e.g., soil properties, water availability, nutrient availability) and influence of management are also important reasons (Schulze et al., 1994). Thus parameter sets, being used for ET modelling, should not only fit plant species and climate zone but should also be representative for special site characteristics. A parameterisation of the PM approach should also consider that parameters alter in dependence on phenological development or physiological state of vegetation. Richter et al. (2015) investigated the benefit of using intra-annual and inter-annual changing parameters in modelling for short rotation poplar plantation. The use of intra-annually and inter-annually changing parameters ruled out the use of parameters derived from literature and resulted in a closer agreement between simulated and measured data.

Genetic variations and different site conditions might be an obvious reason for different parameter sets of the same plant species. However, parameter sets are also affected by the way how they were obtained. Thus, there are inevitable discrepancies between parameters 'directly' determined via porometer measurements and parameters inversely derived from measured ET (Avissar, 1993; Bernhofer, 1993). In the latter case, also the ET measurement method affects the derived parameters. This means derived plant parameters are also influenced by specific uncertainties of the ET measurement method. Additionally, the measurement method used to determine ET also affects the spatial and temporal representativeness of the derived parameters. Parameters used for modelling have to fit the spatial and temporal scale of the specific investigation (Sposito, 2008; Tchiguirinskaia et al., 2004).

Our study addresses the spatial scale of typical agricultural management units (field scale) and is focussed on daily patterns of ET. The main objective is the determination of reliable surface conductance (g_c). In the case of negligible evaporation from the soil one can assume that surface conductance becomes a plant parameter (Monteith, 1965) which can be used to describe transpiration. Today, measurements of ET are often based on eddy-covariance (EC). It is especially focussed on measurement uncertainties affecting the inverse parameter derivation. The effects of energy balance closure, typically occurring in EC measurements (Culf et al., 2004), are analysed and quantitatively assessed. Therefore, the study addresses the error propagation from micrometeorological measurement over parameter determination up to effects on site water balance modelling. Finally, a set of parameters is provided for five different crops (winter barley, winter rape seed, winter wheat, silage maize and spring barley).

2 Material and methods

2.1 Measurement site Klingenberg

Measurements were conducted above an agricultural field (50 ° 54 ′ N, 13 °31 ′ E; 480 m a.s.l.) located at the edge of the eastern Ore Mountains (*Östliches Erzgebirge* in Germany) near *Klingenberg*. The site is part of the Technische Universität Dresden's cluster for greenhouse gas and water fluxes (Moderow and Bernhofer, 2014). It is also part of ICOS (Integrated Carbon Observation Systems, research project funded by the European Union). The measurement site was established in 2004 with the aim to study long-term vegetation-atmosphere-feedbacks. Main objectives are analyses of carbon exchange and carbon balance (e.g., Prescher et al., 2010) as well as investigations of water balance and individual water balance components (e.g., Spank et al., 2013).

The site is situated on a gentle slope facing South-West. The field itself has a shape of an irregular polygon with an extent of 0.8 km (North and South) and 1.1 km (East and West). The field is surrounded by other agricultural fields in the South and North. A village is situated in the West, whereas the easterly border forms a mosaic of grasslands and forests. The measurement station is at the northern margin of the field in flat terrain, fetch is considered to be adequate in all directions. The distance to the northerly border is 0.3 km. The area of the flat terrain expands 0.3 km in North-South and 0.6 km in East-West direction. The test site is positioned in the centre. Thus, the minimum distances are 150 m to the field border in the North and to the nearest group of trees in the South. However, a fetch of more than 300 m can be assumed for both mean wind directions (North-West and South-West).

The climate can be categorized as sub-oceanic/sub-continental. The long-term averages (period 1981–2010) of annual air temperature and annual precipitation, determined at the adjacent climate station 'Grillenburg' (50 °57 ′ N, 13 °31′ E, 385 m above sea level), are 7.8 °C and 901 mm, respectively. Land use and vegetation around the site are characterized by the regionally typical agricultural management of crop rotations. The investigated period (2004–2013) includes two complete 5-years-cycles of yearly changing crop cultures, consisting of winter barley (*Hordeum vulgare*), winter rape seed (*Brassica napus*), winter wheat (*Triticum aestivum*), silage maize (*Zea mays*) and spring barley (*Hordeum vulgare*). The two crop rotation cycles are analysed with regard to the main growing season between 15 April and 15 October. During these periods vegetation height, leaf area index and rooting depth varied with cultivated crops. Furthermore, shorter periods of bare soil occurred after harvest and before seeding.

The soil can be classified as drained Stagnic Umbrisol (FAO soil classification). In the 70ties and 80ties, the field was regularly ploughed after harvest. However, low-tillage is applied since the 90ties. The soil structure still shows characteristic attributable to former ploughing management. Thus, the upper soil layers are a comparably homogenously mixed loamy material. However, layers below of former ploughing zone are significantly more variable in vertical as well as in horizontal dimension; i.e., the material varies between sandy clay and sandy clay loam. Nevertheless, also the upper soil layer exhibits a significant spatial heterogeneity, causing a significant variation of the plant available water within rooting depth. The plant available water ranges between 100 and 170 mm according to field experiments conducted in 2009. It is assumed that limitations of nutrient availability are excluded because of regular fertilisation (organic and inorganic).

2.2 Measurements and EC data post-processing

The station is equipped with an closed-path eddy-covariance (EC) measurements system (more detailed information given below) to observe mass and energy exchange, i.e., fluxes of carbon dioxide (F_{CO2}), water vapour (F_{H2O}) and sensible heat (H) are measured. The evapotranspiration (ET) as well as the latent heat flux (LE) can be derived from measured F_{H2O}. Furthermore, data of momentum flux (τ), wind speed (u), wind direction and friction velocity ($u*$) are provided by the EC-system.

The flux measurements are conducted 3 m above ground. The EC system itself consists of a sonic anemometer (Gill Solent R3, Gill Instruments, UK), a closed-path gas analyser (LI-7000, LI-COR Inc., USA), intake tube (length 7.8 m, diameter 4 mm, flow rate $5\,\mathrm{l\,min^{-1}}$) and a logger unit (PC with interface card). The measurement frequency is 25 Hz. Based on high frequency data, half-hourly fluxes of H, LE, CO_2 and τ are calculated using the software package EdiRe (The University of Edinburgh, 2007). The flux calculation includes three post-processing steps (according to Aubinet et al., 2012): (i) raw data screening (according to Vickers and Mahrt, 1997), (ii) flux calculation and correction and (iii) gap-filling.

Based on raw data, outliers and data beyond absolute limits were eliminated, time lags between wind speed and gas concentration measurements were calculated and the axis rotation for tilt correction was applied (double rotation as described in Wilczak et al., 2001). Calculation of covariances and raw fluxes using half-hourly block averages includes damping correction (Moore, 1986; Leuning and Moncrieff, 1990), sonic temperature correction (Schotanus et al., 1983) and quality assessment (Foken and Wichura, 1996). Further details of the flux processing algorithm as well as information about the sensitivity of individual processing steps can be found in Grünwald and Bernhofer (2007) and Spank and Bernhofer (2008), respectively.

The radiation balance (R_n) as well as its four components (incoming and outgoing short- and longwave radiation) are measured by a net radiometer (CNR 1, Kipp & Zonen, Netherlands). The soil heat flux (G) is measured by two soil heat flux plates (PLE, Laborelektronik Ing. Peter Leskowa, Austria). Air temperature and relative humidity is measured by a humidity moisture probe (HMP 45, VAISALA, Finland). Reflected photosynthetic active radiation is measured by a LI-190SZ (LI-COR, USA). Precipitation is measured by a weighing gauge (Pluvio, OTT, Germany). Soil moisture is recorded via time domain reflectometry (TDR-probe, Trime-EZ, IMKO, Germany) and soil temperatures by self-made thermocouples. The height of vegetation (canopy height, h_c) was routinely measured once per week.

2.3 Reliability and uncertainty of measured flux data

2.3.1 Effects of post-field data processing

Currently, the eddy covariance technique is assumed to be the most exact micrometeorological method to observe mass and energy exchange (Foken, 2008). Nevertheless, estimated fluxes can be seriously affected by specific measurement uncertainties. The uncertainty of EC flux measurements, i.e. uncertainty of half-hourly flux data, are a result of complex interdependencies between hardware characteristics and flux processing algorithms which are themselves complexly interfere with meteorological conditions (Mauder et al., 2007). At the present time, methods are not available for an operational quantitative uncertainty assessment of half-hourly flux data. Thus, evaluation of half-hourly EC data is typically based on qualitative assessments as described by, e.g., Foken and Wichura (1996) or Mauder et al. (2013).

Our study addresses the daily time scale where random uncertainties of half-hourly records are attenuated. However, systematic under-, or overestimations are preserved (Moncrieff et al., 1996) and often aggregated to remarkable values. This systematic uncertainty is significantly affected by the approach of EC flux processing. Mauder et al. (2007) compared different methods of flux processing. They found that different post-field processing schemes can cause differences up to 15 % in the estimated latent heat flux. Our own analyses indicate (unpublished results) that this uncertainty is in a range between 5 and 10 % for presented daily estimates of LE and typical weather conditions.

The problem of data gaps in EC flux data is another special point that has to be regarded. Data gaps cannot be avoided and are caused by a variety of reasons, e.g., EC measurements fail in unfavourable weather conditions (e.g., very stable atmospheric stratification, heavy rainfall and fog), or measurements are interrupted by issues of maintenance. However, different strategies for gap filling exists which lead in turn to significant differences in long-term balances (Falge et al., 2001a; Falge et al., 2001b, Moffat et al., 2007). In our study, gaps in the half-hourly flux record have been filled using the eddy covariance gap-filling and flux-partitioning tool (Reichstein et al., 2005). However, for analyses presented here, only days were used where the total time of missing data was less than 4 hours per day and a continuous data gap was not longer than 2 hours. Tests of this proceeding have shown that the uncertainty caused by filling of two-hour data gaps is smaller than 5 % for daily estimates of LE and ET. Thus, it can be concluded that effects of gap filling have minor importance for our investigations.

2.3.2 Footprint

EC measurements provide data of the turbulent exchange from an area, called footprint (Foken, 2008). The dimension of the footprint and the spatial weighting of signals within footprint depend on site parameters, i.e., measurement height and height of vegetation, and meteorological variables, i.e., atmospheric stratification, wind speed, and wind direction (Rannik et al., 2012). Therefore the dimension of the footprint varies with changing meteorological conditions and site characteristics in time and space (Leclerc and Foken, 2014). We assessed the footprint using the methodology of Klujn et al. (2004). The footprint's dimension varies between 50 and 150 m in longitudinal direction of wind for typical weather condition and typical daily pattern of meteorological variables. This means that measured fluxes mainly originate from the target area under typical weather conditions.

The crop can be assessed to be widely homogeneous within the footprint area. Noticeable differences in phenological state, vegetation height or discrepancies in the (visually recognisable) fitness of plants have not been observed. Notwithstanding, soil properties differ within the footprint. Different soil properties could cause a small scale variability of crop's transpiration behaviour. However, as neither fitness nor height of plants confirms such heterogeneity, we assume that effects of soil's heterogeneous properties can be neglected here. Besides this, one can assume that the plant cover was very homogenous at all times as the respective field is conventionally managed, i.e., the management is selected in such a way that only the grown crop benefits from it and other plants are suppressed.

2.3.3 Energy balance closure gap

The 'energy balance closure gap' (EBCG) is another important item – one has to consider when EC measurement data are used for analyses of ecosystem exchange (Culf et al., 2004). EBCG denotes an imbalance between the right ($H + LE$) and left ($R_n - G$) side of the energy balance equation (Eq. (2.1)),

$$R_n - G = H + LE, \tag{2.1}$$

which is mainly caused by systematic underestimations of fluxes measured via EC technique. The EBCG is a well-known phenomenon and has been investigated in numerous studies (e.g., Wilson et al., 2002a; Wilson et al., 2002b; Barr et al., 2006; Oncley et al., 2007; Panin and Bernhofer, 2008; Moderow et al., 2009; Franssen et al., 2010; Stoy et al., 2013).

The reasons of EBCG are mainly attributed (i) to technical imperfections of the measurement set-up and (ii) to undetected non-turbulent fluxes (Foken et al., 2011; Leuning et al., 2012). The second point means that only turbulent fluxes of mass and energy exchange are measured by the EC technique. However, transport processes via diffusion and advection remain unobserved. These two major reasons for the systematic underestimation of the 'actual' flux exchange are overlaid by uncertainties caused by post-field data processing and uncertainties inherent in the assessment of the available energy (discussed below). However, it should be noted that both – effects of post-field data processing and uncertainties of available energy – cannot be the only reason for the EBGC as explained by Mauder et al. (2007) and Moderow et al. (2009), respectively. Thus, the EBCG provides a conservative quantity encircling the range of physical plausibility for measured daily LE and ET (see Section 2.5.).

2.4 Energy storage and quantification of available energy

The storage changes (ΔS) have been neglected in Eq. (2.1) as effects of ΔS widely compensated on daily scale which is the study's time scale of investigation. However, daily values are derived from samples of half-hourly data. Thus storage changes have to be considered to avoid potential errors. If storage changes are not neglected Eq. (2.1) becomes:

$$R_n - G - \Delta S = H + LE. \tag{2.2}$$

The left hand side of Eq. (2.2) is often referred to as available energy (AE). We will use this term throughout the whole paper,

$$R_n - G - \Delta S = AE. \tag{2.3}$$

The storage change was calculated as the total of three components (Eq. (2.3)):

$$\Delta S = \Delta S_H + \Delta S_L + \Delta S_B. \tag{2.4}$$

where ΔS_H denotes changes of sensible heat storage and ΔS_L changes in the latent heat storage (both between ground level and EC-measurement height). ΔS_B denotes heat storage changes in the biomass. It should be noted that energy fluxes due to chemical use or release is ignored here, as they are typically small.

The methods to determine ΔS_H, ΔS_L, and ΔS_B are described in Bernhofer et al. (2003). ΔS_H and ΔS_L can be directly derived from measured variables. ΔS_H

and ΔS_L are computed from differences of air temperature ΔT_a and differences of air humidity (change of water vapour density in ambient air, $\Delta\rho_v$), respectively, between previous and subsequent half-hourly time step (Δt) by,

$$\Delta S_H = \rho_a c_p z_m \frac{\Delta T_a}{\Delta t} \quad (2.5)$$

and,

$$\Delta S_L = L\, z_m \frac{\Delta\rho_V}{\Delta t}, \quad (2.6)$$

respectively, where ρ_a denotes density of air ($\approx 1.2\,\mathrm{kg\,m^{-3}}$); c_p, heat capacity of air at constant pressure ($\approx 1005\,\mathrm{J\,kg^{-1}\,K^{-1}}$); L, latent heat of evaporation ($\approx 2.5 \cdot 10^6\,\mathrm{J\,kg^{-1}}$); and z_m, measurement height (3 m above ground level). However, routine computation of ΔS_B requires several assumptions and simplifications as actual drivers are not routinely measured. According to Bernhofer et al. (2003), ΔS_B can be approximated by,

$$\Delta S_B = c_b\, m_v \frac{\Delta T_b}{\Delta t}. \quad (2.7)$$

The soil temperature (measured 2 cm below the surface) is a good approximation for the temperature of biomass (T_b). The heat capacity of biomass (c_b) can be approximated by $1.7 \cdot 10\,\mathrm{J\,kg^{-1}\,K^{-1}}$, and the mass of vegetation (m_v) can be rated via a linear regression to vegetation height (h_c) by,

$$m_v = 0.8\, h_c. \quad (2.8)$$

(m_v in kg and h_c in m). As ΔS_B is typically more than a magnitude smaller than ΔS_H and ΔS_L for the investigated crop site, uncertainties, caused by this rough approximation of ΔS_B, are insignificant in relation to the total of ΔS.

2.5 Reference and plausible upper and lower limits for estimated daily values of ET and LE

In our study, the systematic characteristic of EBCG provides the basis to obtain measuring tolerances for estimated daily values of ET and LE. If one accounts for ΔS then the EBCG is still 30 % of the available energy on average (based on half-hourly data of the investigated period here). This is a typical value for EBCG of agricultural sites according to results of Wilson et al. (2002a) and Franssen et al. (2010). Nevertheless, it should be noted that energy balance closure is highly variable at half-hourly time scale and also periods of 'over-closure' ($H + LE > AE$) could be observed. The phenomenon of EBCG occurs also at larger time scales, e.g. days. However, EBGC cause a clear one-sided bias ($H + LE < AE$) here.

As the actual mass and energy exchange is systematically underestimated by EC measurements, the physical lower limits of daily LE and ET can be directly derived from the measured water vapour flux. This lower bound of plausibility is referred here to as LE_{EC} and ET_{EC}. The upper bounds of ET and LE can be obtained from energy balance using Eq. (2.9),

$$LE = AE - H. \quad (2.9)$$

This means that the missed energy and therewith the amount of EBCG is totally attributed to LE which implies that H is correctly determined. There is an ongoing discussion to whether LE and H are underestimated by EC-measurements to the same degree or not (e.g., Barr et al., 2006; Mauder and Foken, 2006; Stoy et al., 2006; Wohlfahrt et al., 2010; Ingwersen et al., 2011; Mauder et al., 2013; Charuchittipan et al., 2014; and Eder et al., 2014). Nevertheless, this approach (Eq. (2.9)) provides a defensible way to determine plausible upper bounds for daily values, being called LE_{EB} and ET_{EB} hereinafter.

Estimates LE_{EB} and ET_{EB} could be significantly affected by uncertainties of AE (Spank et al., 2013). Uncertainties of daily AE are mainly caused by uncertainties of measured net radiation (R_n). However, effects caused by uncertainties of G and ΔS can be neglected as both are characterised by positive values during day and negative values during night which compensate each other at a daily time scale. There are several studies which compared different net radiometers measurements at sub-daily time scales, e.g., Halldin and Lindroth (1992), Vogt et al. (1996) and Kohsiek et al. (2007). Halldin and Lindroth (1992) stated an uncertainty of the investigated net radiometers of ±3.5 % in relation to their reference instrument. Kohsiek et al. (2007) compared net radiometers of the type CNR1 (Kipp & Zonen, Netherlands) to the reference sum of four components and yielded similar uncertainties as Halldin and Lindroth (1992). Vogt et al. (1996) assume an uncertainty of ±3.5 % or $6\,\mathrm{W\,m^{-2}}$ (whichever was largest) based on own intercomparison experiments but also in relation to Halldin and Lindroth (1992). The total uncertainty of available energy was assessed by Vogt et al. (1996) and Moderow et al. (2009) amongst others. Moderow et al. (2009) state an average uncertainty of AE of approximately 12 %. Vogt et al. (1996) stated a smaller value of 6 % around midday. All studies agree that uncertainties of AE affect the quantity of EBCG. However, it is also clearly emphasised by these studies that the EBCG cannot be explained by the uncertainty of AE alone. That means, even in the worst case, daily values derived via Eq. (2.9) would overestimate the 'actual' flux. Thus LE_{EB} and ET_{EB} can be taken as robust conservative estimates for the physical upper bound.

Additionally to the physical lower bound (LE_{EC} and ET_{EC}) and the physical upper bound (LE_{EB} and ET_{EB}), reference values (ET_{Ref} and LE_{Ref}) were calculated according to Blanken et al. (1997). The methodology is based on a weighted allocation of EBCG via Bowen's ratio (β),

$$\beta = \frac{H}{LE}. \qquad (2.10)$$

In doing so, one assumes that β is the same as for the measured fluxes, i.e., scalar similarity is preserved. However, several studies (e.g., Wilson et al., 2002b; Asanuma et al., 2007; Barr et al., 2006; Ruppert et al., 2006; Foken et al., 2011; Charuchittipan et al., 2014) question this assumption. Furthermore, also effects of post-field data processing and, particularly, uncertainties caused by uncertainties of estimated daily AE have to be kept in mind.

As discussed above, the method to partition the remaining energy (EBCG) to the turbulent fluxes of H and LE using β bears some uncertainties. Twine et al. (2000) tested this method using data of six grassland and two crop sites. Their results showed that the method to partition EBCG using β produces more reliable estimates of LE (and ET) than those given by LE_{EC} (ET_{EC}) or LE_{EB} (ET_{EB}). Spank et al. (2013) demonstrated that this methodology is also suitable for the site investigated here. However, we want to point out that the methodology was not used to provide a "best guess" for the unknown actual values of LE and ET but as a confident reference which is located between LE_{EC} (ET_{EC}) and LE_{EB} (ET_{EB}).

2.6 Penman-Monteith approach

The PM approach (Monteith, 1965) facilitates the estimation of ET. It is a further development of Penman's approach (Penman, 1948) which links the energy balance with flux-gradient relationships of H and LE. The novelties of PM approach compared to Penman's original were the introduction of an additional parameter named canopy resistance (r_c), which describes the plant physiological reactions to meteorological conditions, and the implementation of the aerodynamic resistance (r_a), which replaced the undefined wind function in Penman's original approach. The 'standard form' of the PM model is commonly given as follows (Monteith, 1990),

$$LE = \frac{s\,(T_a)\,(R_n - G) + \rho_a c_p \frac{e*(T_a)-e}{r_a}}{s\,(T_a) + \gamma \frac{r_a + r_c}{r_a}}, \qquad (2.11)$$

where ρ_a denotes density of wet air; c_p, specific heat of air at constant pressure ($c_p \approx 1005\,\mathrm{J\,kg^{-1}\,K^{-1}}$); γ, psychrometer constant ($\gamma \approx 0.622\,\mathrm{hPa\,K^{-1}}$); and where air temperature T_a already replaces T_s (leaf surface temperature) assuming sufficient coupling between leaf and ambient air.

For practical application, it is often necessary (as in our case) to consider ΔS for a correct definition of the available energy. Consequently, the term $(R_n - G)$ is substituted by AE. Substituting of r_c and r_a by their reciprocals canopy conductance ($g_c = r_c^{-1}$) and aerodynamic conductance ($g_a = r_a^{-1}$) and substitution of $e*(T_a) - e$ by vapour pressure deficit (VPD) alters Eq. (2.5) to,

$$LE = \frac{s\,(T_a)\,AE + g_a \rho_a c_p VPD}{s\,(T_a) + \gamma \left(1 + \frac{g_a}{g_c}\right)}, \qquad (2.12)$$

This equation can be rearranged to inversely determine g_c based on measurements of LE and determinations of g_a based on measured data (Eq. (2.14)),

$$g_c = \frac{g_a}{\frac{s(T_a)}{\gamma}\frac{AE-LE}{LE} - \frac{g_a \rho_a c_p VPD}{\gamma LE} - 1}, \qquad (2.13)$$

It should be noted that the PM approach was originally developed for closed canopies. However, several hydrological studies have shown that the approach is also suited to simulate ET of canopies with canopy gaps provided that when g_c has been accordingly adapted. If soil evaporation is an important component of ET then it is more correct to use the term 'surface conductance' instead 'canopy conductance'. As the methodology is identical to determine both variables, we keep the abbreviation of g_c.

2.7 Determination of aerodynamic conductance

The flux-gradient relationships of H and LE, which provide the basis for the PM approach, use the aerodynamic resistance of heat exchange (r_{aH}) and aerodynamic resistance of vapour exchange (r_{aV}) respectively. However, the majority of exchange occurs in atmospheric boundary layer by turbulent transport, i.e., the overwhelming exchanges of heat and mass takes place via defined air parcels called eddies (Shuttleworth, 2012). It is a reasonable assumption (Foken, 2008) that eddies similarly transport both heat and mass (e.g., water vapour). Thus, r_{aH} and r_{aV} can be equalised to r_{aHV}. The value of r_{aHV} is complexly determined by wind speed u, atmospheric stability, roughness height z_0, zero plane displacement z_d and thickness of viscous sublayer. However, according to Monteith (1990), r_{aHV} can be approximated by the aerodynamic resistance r_{aM} of momentum flux when the effect of the boundary layer resistance, addressing the diffusion through the viscous sublayer, can be neglected or can be treated as part of r_c. One can further reasonably assume that effects of atmospheric stability are widely compensated on daily time scale. Therefore, r_a can be directly derived from EC measurements using measured wind speed (u) and friction velocity (u*),

$$r_a \approx r_{aM} = \frac{u}{u*^2}. \qquad (2.14)$$

2.8 Data sets used to determine daily canopy conductance

The primary goal of the study presented here is to obtain representative values of daily canopy conductance g_c for simulation of transpiration at field scale. Days, where precipitation was recorded, were excluded from analyses. Furthermore, days were excluded when data gaps in the half-hourly sub-records could not be filled by the gap filling procedure. In the same way, also days were declined when total of gap-filled half-hourly records was longer than 4 hours per day or duration of continuous gaps was longer than 2 hours. The dataset obtained by this procedure is referred to as dataset (i) hereinafter. However, many days have to be discarded in dataset (i) due to the imposed restrictions. This in turn did not allow to assess seasonal pattern of g_c sufficiently. Furthermore, effects of non-recorded precipitation events of low intensity and quantity as well as dew evaporation cannot be excluded in this way.

To avoid these drawbacks, daily values of g_c were additionally determined from average daily curves, being derived from dry (rainless) half-hourly data. The half hourly data of R_n, G, ΔS, H, LE, T_a, e, u and $u*$ were filtered as follows: measured P(half-hourly total) = 0 mm, $VPD \geq 1$ hPa, and $RH \leq 90$ %. Additionally, we considered that the canopy is wet for some time after precipitation. Therefore, data recorded within 3 (5) hours after the end of the precipitation event were excluded during daytime (nighttime). The separation of day and night is based on a threshold for solar radiation of 5 W m^{-1}. As a result, samples of half hourly data were created, being widely unaffected by precipitation and interception. These 'rainless' data were continuously used to calculate average daily courses within a moving time window of +/−5 days. These averages daily courses were temporally integrated to create 'virtual rainless days'. Subsequently, g_c was determined via Eq. (2.13) from these 'virtual rainless days'. This dataset is denoted as dataset (ii) hereinafter.

Therefore we used two datasets to determine g_c: (i) dataset of rainless days and (ii) dataset based on average daily courses of rainless periods and further filtered for conditions indicating a possible wet canopy, hereinafter. The surface conductance obtained using these data sets are accordingly labelled g_c(i) and g_c(ii), respectively. The effects of the energy balance close gap (EBCG) on estimates of g_c are a special focus of this study. As noted above, EBCG is utilized here as a tool to define in which range of physically reliable values the measured water vapour flux should be (see Section 2.5). Accordingly, the lower limit of g_c results from LE_{EC}, hereinafter $g_{c,EC}$, and the upper limit from LE_{EB}, hereinafter $g_{c,EB}$. A reference value ($g_{c,Ref}$) was determined by the usage of LE_{Ref}.

2.9 Determination of periods with maximum canopy conductance

An important object of our study is the assessment of maximum surface conductance ($g_{c,\max}$) which should be representative for maximum transpiration of plants during vegetation periods. This parameter is required in numerous water balance models and has therefore highly practical relevance. Care should be taken when $g_{c,\max}$ is directly derived from annual curves of g_c because g_c of bare wet soil as well as outliers could take similar or even larger values. Thus, an indicator is required, which marks periods that are suitable for obtaining values of $g_{c,\max}$. Unfortunately, well-defined variables, i.e., LAI (leaf area index) and BBCH code, assessing plant's fitness and phenological development, are not continuously observed. (The BBCH code system is a sophisticated and accepted method to uniformly classify the different phenological development stages of mono- and dicotyledonous plant; for further details see JKI, 2015.) Thus, a proxy is required. The canopy height (h_c) is often used in the hydrological praxis therefor. However, as our results (presented in Section 3.1) clearly demonstrate, this proceeding leads to misleading results. Consequently, another variable is required for the separation of periods with highest plant activity (PHPA) and for determination of $g_{c,\max}$.

The light use efficiency (LUE) is a reliable indicator to assess plant's activity and productivity related to carbon fixation. Our study does not address carbon exchange; however, LUE is used as proxy to assess plant's fitness and phenological state. I.e., daily values of LUE are used in combination with measured h_c to separate phases of high and low activity. In our study, LUE is defined as ratio between daily gross primary production (GPP, derived from measured F_{CO2}) and daily value of measured incoming photosynthetic active radiation (PAR),

$$LUE = \frac{GPP}{PAR}, \tag{2.15}$$

For determination of $g_{c,\max}$, periods were selected where the moving average (+/−5 days) of LUE does not fall below 80 % of annual maximum ($LUE_{\max}$). The representative value of $g_{c,\max}$ was continuously assessed by period's average of daily g_c (ii). This proceeding was necessary to compensate weather induced variations as well as to minimize possible effects due to measurement uncertainties, data gaps and possibly periods where the canopy was wet. The threshold of 80 % (0.8 $LUE_{\max}$) was assessed based on results of a sensitivity analysis. It was found that a thresholds between 70 % and 90 % of $LUE_{\max}$ provides representative values for $g_{c,\max}$. This means determined $g_{c,\max}$ varied by less than 10 % when the threshold was varied between 70 % and 90 % $LUE_{\max}$. Thus, 'random' fluctuations are compensated; however, representativeness of maximum is not corrupted due to long averaging periods. Ultimately, 80 % of $LUE_{\max}$ was taken as a fair compromise.

2.10 Test of Reliability and Representativeness of obtained $g_{c,\max}$

Determined values of $g_{c,\max}$ based $g_{c,Ref}$ (shown in Fig. 3) were inserted in Eq. (2.12) and were used to calculate LE and subsequently ET. The simulations were driven by meteorological data of dataset (i). Simulated daily estimates of ET (ET_{Mod}) were compared to measured daily estimates of ET for rainless days within PHPA, i.e., ET_{Ref} of dataset (i) were used for the evaluation. However, it should be noted that PHPA was assessed in contrast to the general proceeding (0.8 LUE_{max}) by 0.7 LUE_{max} for the years 2012 and 2013, as the number of rainless days using a selection criterion of 0.8 LUE_{max} was too low for these years, i.e. only 9 and 8 days, respectively, would have been selected.

The agreement between simulation and measurement was evaluated using the coefficient of determination (R^2), the bias and the bias corrected root mean square error ($RMSE_b$). R^2 assesses how well relative courses of measurement and simulation agree. A value of $R^2 = 1$ means that both curves are absolutely synchronous. However, R^2 does not detect a potential offset between both curves. Unlike that, the bias evaluates such an offset. Thus, it evaluates the accuracy of simulation and therewith the systematic difference between ET_{Mod} and ET_{Ref}. Complementarily, $RMSE_b$ assesses the scattering or the random component of the deviation between ET_{Ref} and ET_{Mod}, i.e., the precision is evaluated.

As data for two cycles of crop rotation are available, two different simulations were run. The first one (Sim_A) utilizes the year specific obtained value of $g_{c,\max}$. Here, it should be kept in mind that almost identical data set were used to derive $g_{c,Ref}$ and for test data of ET_{mod}. Thus effects of an inappropriate parameterisation of g_c are minimized in Sim_A. Consequently, the difference between ET_{Mod} and ET_{Ref} is almost exclusively caused by (1) imperfections of model, (2) data uncertainties (meteorological input and ET_{Ref}), (3) uncertainties in estimates of r_a, and (4) low-pass filtering introduced in the process of obtaining $g_{c,\max}$. Thus, Sim_A can be used to assess the site specific background uncertainty of the PM approach. For the second simulation (Sim_B), estimates of $g_{c,\max}$ were exchanged between the two crop rotation cycles, i.e. $g_{c,\max}$ of the first crop rotation period were used for simulation of the second crop rotation period and vice versa. This allows an evaluation of the representativeness of obtained $g_{c,\max}$. Furthermore, effects of obtained $g_{c,\max}$ on ET_{Mod} could be assessed with respect to background uncertainty.

3 Results

3.1 Annual curve course of g_c and effects of EBCG

Calculated values of canopy conductance g_c are shown in Fig. 1 for the main growing season (15 April until 15 October). Corresponding crops of both crop rotation cycles are compared for comparison. Fig. 1 shows g_c calculated from data set (i) and data set (ii). Additionally, the canopy height (h_c) is displayed in the background for orientation. It was not possible to obtain continuous courses of g_c(i) as consecutive days of rain often cause long lasting data gaps. Thus, only days are displayed when g_c(i) was actually computable. The whiskers indicate the range between $g_{c,EC}$ and $g_{c,EB}$, and the cycle symbol in between represents $g_{c,Ref}$. Almost continuous courses of g_c could be obtained from data set (ii) which are presented in the same way in Fig. 1. The courses of g_c(ii) and data points of g_c(i) do widely agree, i.e., the range between $g_{c,EC}$ and $g_{c,EB}$ partly coincides with g_c(i) and g_c(ii). Only individual outliers are observable for g_c(i) and are likely caused by non-recorded, small events of precipitation.

The effects of EBCG on estimated g_c have a similar characteristics for data set (i) and data set (ii). Largest differences between $g_{c,EB}$ and $g_{c,EC}$ occur in periods of largest g_c. This behaviour can be easily explained when looking at Eq. (2.13). Differences between $g_{c,EB}$ and $g_{c,EC}$ will increase when differences between LE_{EB} and LE_{EC} increase as large values of LE leads to a smaller denominator. High values of LE typically occur during day where the absolute magnitude of the energy balance gap is largest (e.g., Lindroth et al., 2010) Thus, differences between $g_{c,EB}$ and $g_{c,EC}$ become larger in periods of high exchange rates.

3.2 Interdependency of g_c, h_c and LUE

Fig. 1 also shows that the relative courses of g_c and h_c do not agree with each other. In the beginning of the growing season g_c increases with h_c but g_c decreases with the beginning of ripening. However, a significant discrepancy is apparent before the onset of the ripening stage, i.e. maxima or least very large values of g_c are already reached before the maximum of h_c occur. This means plants still grow and biomass increases; but g_c does not alter much or even decreases. Maize (year 2012) and rape seed (year 2010) are well defined examples for this. Furthermore, large values of g_c could be observed during periods with bare soil and during periods when the soil is only partly covered with vegetation, i.e. g_c can take values as large as for highly active plants during those periods.

It can be easily concluded that large uncertainties of $g_{c,\max}$ of the inspected crop can occur if it is not properly accounted for periods with only evaporation from bare soils or for periods with a wet canopy as $g_{c,max}$ for these situations can take values as large as for highly active plants. This means that $g_{c,\max}$ cannot be simply derived from annual courses. Additionally, the occurrence of $g_{c,\max}$ in time does not coincide with the occurrence of highest h_c in time which suggests differences in the annual course between these two characteristics. Therefore, h_c is not the best proxy to determine times of $g_{c,\max}$. Under such circumstances, LUE is a more suitable proxy to asses plant activity and times when $g_{c,\max}$ occurs (Fig. 2). Fig. 2 clearly shows the differences in the annual courses of $g_{c,\max}$ and h_c but shows a nicely synchronous behaviour of LUE and transpiration. This means that LUE and courses of LUE can be used as proxy to localize PHPA.

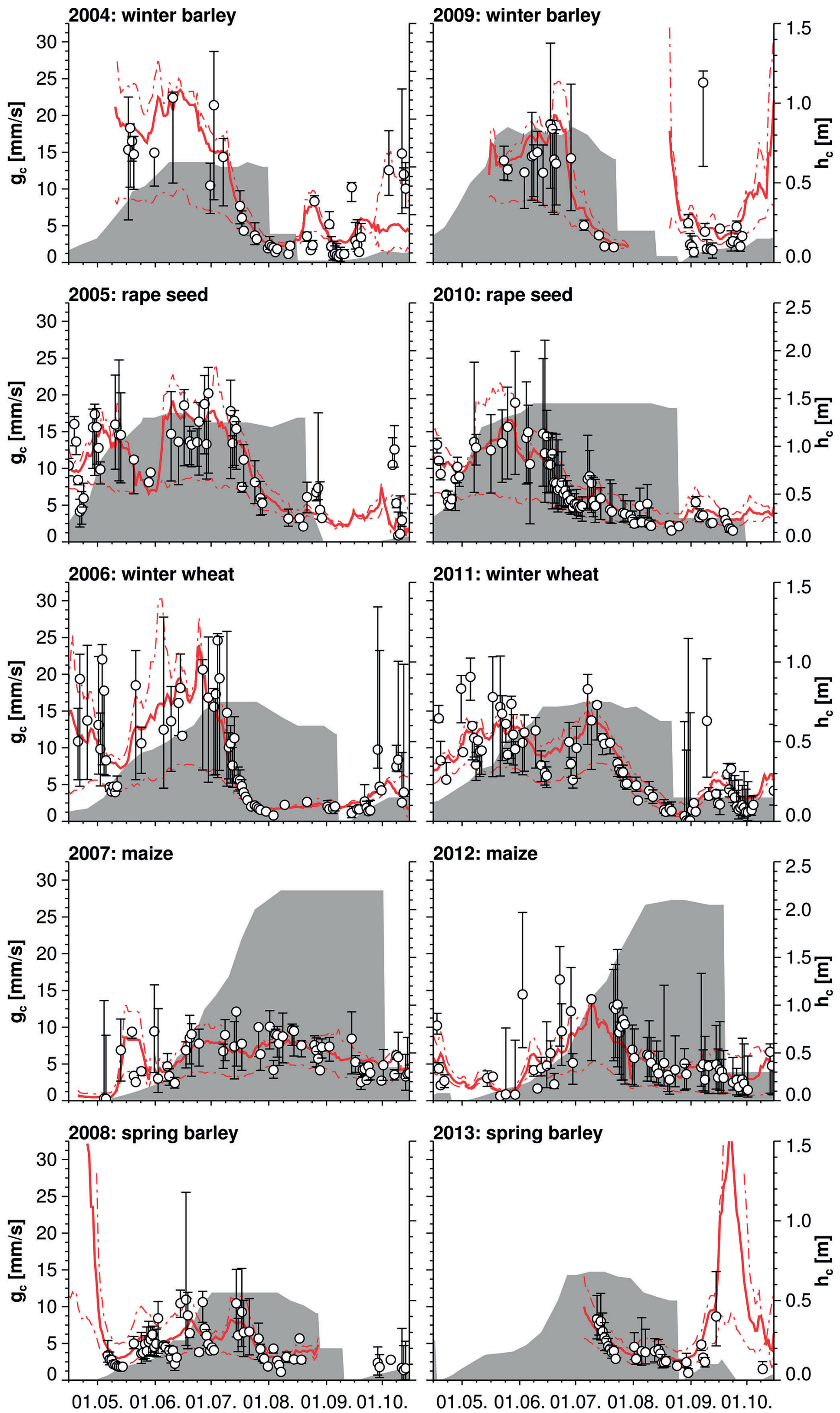

Figure 1: Estimated values of surface conductance g_c and measured canopy height h_c for the main growing season (15 April until 15 October); open circles: $g_{c,Ref}$, whiskers: $g_{c,EB}$ (upper limit) and $g_{c,EC}$ (lower limit) calculated from data set (i); solid red line: $g_{c,Ref}$, dash-dotted red line: $g_{c,EB}$ (upper line) and $g_{c,EC}$ (lower line) calculated from data set (ii); shaded area: h_c.

Furthermore, Fig. 2 also suggests that LUE is a reliable parameter to distinguish between periods, where ET is dominated by transpiration, and periods, where ET is dominated by evaporation from soil and litter (harvest residues). Similar high values of g_c in May 2007 or October 2012 are correctly indicated as periods of high soil evaporation as LUE is low but g_c shows quite high values. Within these periods, the field has been already harvested and the surface was predominantly characterised by bare soil and therefore; ET originated mainly

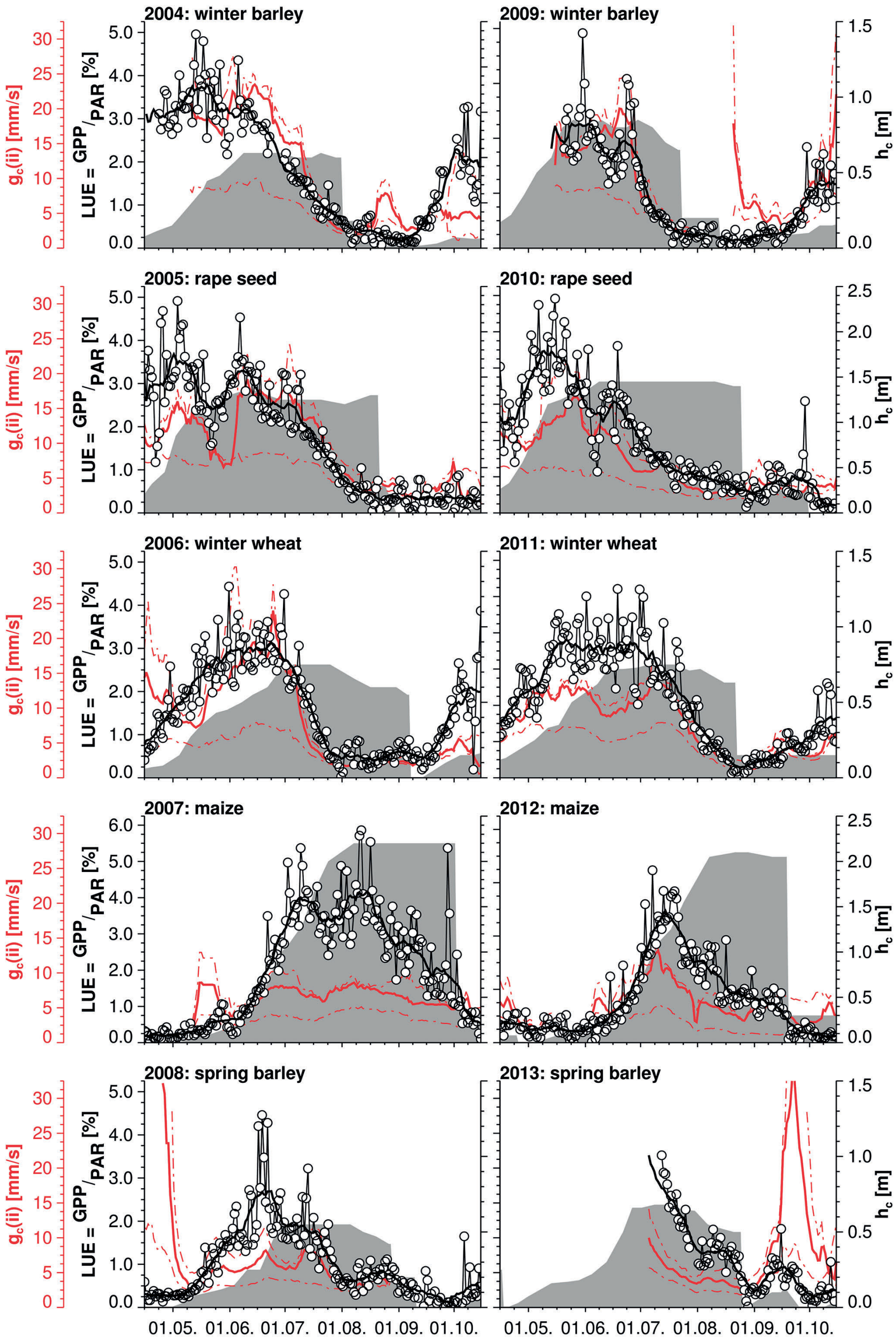

Figure 2: Annual courses of canopy height h_c, light use efficiency LUE and surface conductance g_c calculated from data set (ii) for the main growing season (15 April until 15 October); open circles: daily value of LUE; solid black line: moving average (+/−5 days) of daily LUE; red lines refer to g_c(ii); solid red line: $g_{c,Ref}$, dash-dotted red line: $g_{c,EB}$ (upper line) and $g_{c,EC}$ (lower line); shaded area: h_c.

from bare soil and litter. However, high values of g_c in October 2006 and October 2011 could be observed as new vegetation developed due to self-sowing and/or weed infestation. This is indicated by relative high values of LUE and similar courses of g_c and LUE. A third example might be the period of September-October in 2013. Here, unusual high values of g_c are caused by a superposition of transpiration (re-greening) and high evaporation (litter), a situation where the surface was characterised by a mosaic of newly grown plants, bare soil and litter. The contribution of plant activity to ET is indicated by moderate values of LUE.

3.3 Representative maxima of canopy conductance

Fig. 3 shows the median of $g_{c,Ref}$ (dataset ii) within PHPA corresponding periods of crop rotation are paired in order to facilitate comparison. Additionally, the upper

Table 1: Arithmetic Average, Standard Deviation, Median as well as 10 %, 25 %, 75 % and 90 % percentile of $g_{c,Ref}$ within period of highest plant activity (PHPA); values in brackets are the same statistical quantities, however, calculated for $g_{c,EC}$ (first item) and $g_{c,EB}$ (second item); all values of g_c calculated from data set (ii).

Crop	**Year**	Arithmetic Average	Standard Deviation	**Percentile**				
				10 %	25 %	**50 % (Median)**	75 %	90 %
winter barley	2004	19.2 (8.7, 23.4)	1.7 (0.4, 1.9)	17.3 (8.1, 21.1)	18.1 (8.4, 21.8)	18.6 (8.7, 23.7)	20.7 (9.1, 24.4)	21.5 (9.3, 26.0)
	2009	16.0 (8.0, 18.1)	2.0 (0.6, 3.0)	13.1 (7.0, 14.2)	14.1 (7.5, 15.5)	16.2 (8.1, 18.1)	17.2 (8.5, 19.1)	19.2 (8.7, 24.3)
rape seed	2005	12.3 (7.6, 13.8)	3.4 (0.6, 4.4)	7.3 (6.8, 7.9)	9.7 (7.0, 10.2)	12.7 (7.5, 13.7)	14.6 (8.0, 16.2)	17.0 (8.3, 20.3)
	2010	13.1 (6.2, 17.4)	2.3 (0.3, 4.1)	9.7 (6.0, 10.3)	10.9 (6.0, 12.4)	13.3 (6.2, 19.4)	15.4 (6.5, 20.2)	16.6 (6.6, 20.9)
winter wheat	2006	16.5 (6.7, 20.6)	2.7 (0.9, 4.1)	12.8 (5.5, 16.0)	14.5 (5.8, 17.3)	16.2 (7.0, 20.4)	18.1 (7.3, 22.9)	19.5 (7.7, 27.3)
	2011	11.2 (6.4, 12.6)	1.4 (0.8, 1.4)	9.1 (5.3, 10.6)	10.0 (5.6, 11.5)	11.3 (6.5, 12.5)	12.4 (7.1, 13.8)	13.0 (7.3, 14.3)
maize	2007	7.4 (4.2, 8.0)	0.7 (0.7, 1.0)	6.5 (3.2, 6.6)	6.8 (3.5, 7.3)	7.6 (4.5, 8.1)	7.9 (4.8, 8.5)	8.2 (5.0, 9.6)
	2012	8.5 (3.6, 9.2)	2.7 (1.3, 2.5)	5.4 (1.9, 6.1)	5.9 (2.1, 7.1)	8.5 (3.8, 9.2)	10.5 (4.8, 11.2)	12.4 (5.2, 12.7)
spring barley	2008	7.0 (3.9, 9.7)	0.7 (0.3, 1.1)	6.2 (3.4, 8.3)	6.6 (3.7, 8.9)	7.0 (4.0, 9.7)	7.4 (4.2, 10.3)	8.0 (4.4, 11.1)
	2013	6.2 (4.2, 8.3)	1.1 (0.5, 1.7)	5.1 (3.6, 6.6)	5.5 (3.9, 7.1)	6.0 (4.1, 7.9)	7.1 (4.6, 9.8)	7.8 (5.1, 10.9)

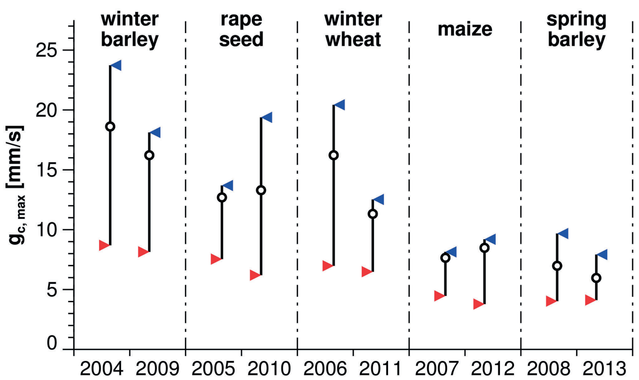

Figure 3: Median of surface conductance g_c within period of highest plant activity; red triangle: $g_{c,\max}$ derived from $g_{c,EC}$; open circle: $g_{c,Ref}$; blue triangle: $g_{c,EB}$; all values of g_c calculated from data set (ii).

($g_{c,EB}$) and lower limits ($g_{c,EC}$) of g_c are shown which result from the different handling of the EBCG. The wide span between $g_{c,EC}$ and $g_{c,EB}$ causes that differences between different crops are blurred. However, $g_{c,Ref}$ of a distinct crop of different years is typically within the range of $g_{c,EB}$ and $g_{c,EC}$ regardless for which year these limits where determined (with exception of winter wheat in 2006). Thus, the upper ($g_{c,EB}$) and lower limits ($g_{c,EC}$) can be used to identify the range in which $g_{c,\max}$ can be expected for the respective crop. Furthermore, Fig. 3 allows a qualitative ranking of $g_{c,\max}$; from low to high g_c: spring grain (spring barley and maize), rape seed, winter grain (winter wheat and winter barley). For better overview and for reason of completeness, all variables, shown in Fig. 3, are additionally itemized in Table 1. Additionally, the most important statistical key values describing the statistical distribution of g_c within PHPA, i.e., 10 %, 25 %, 75 % and 90 % percentile, arithmetic average and standard deviation, are listed.

Fig. 3 also indicates the sensitivity of g_c on uncertainties of LE. The average differences between $g_{c,EC}$ and $g_{c,Ref}$, and between $g_{c,Ref}$ and $g_{c,EB}$ are 5.7 mm s^{-1} and 2.5 mm s^{-1} respectively for PHPA. The medians of the relative differences are 46 % and 19 %, respectively, which demonstrates that the EBCG has an enormous impact on computed numerical value of g_c. It should be noted that the EBGC was only 19 % on average for periods used to determine $g_{c,\max}$. However, EBCG is approx. 30 % on average, if complete periods (15 April until 15 October) are regarded. Thus, it can be concluded that effects are even higher for other periods than for periods which have been used to determine $g_{c,\max}$.

The strong impact of EBCG on estimates of $g_{c,\max}$ supports the statement that the applied method to determine ET or LE has significant impact on the obtained value of g_c as well as its representativeness. In that way, different values of g_c between different authors can be also explained by methodological differences. This fact is particularly important when different sites or different types of land use are compared. In case of EC measurements, the EBCG has to be considered as a major source for uncertainties. Related effects weaken the representativeness of calculated g_c and restrict direct comparability. Thus, reasonable conclusions can be only drawn based on comparisons which consider uncertainty of inputted LE and confidence range of obtained g_c.

3.4 Results and evaluation of tests for reliability and representativeness of $g_{c,\max}$

Fig. 4 and 5 show the bias and $RMSE_b$, respectively, for Sim_A and Sim_B. Each plot shows the respective variable in mm d^{-1} (upper diagram) and in % (lower diagram). A visualization of R^2 is omitted here as R^2 was always greater than 0.8 for all simulations and differences of R^2 were negligible between Sim_A and Sim_B. The high values of R^2 indicate the general suitability of the PM approach for the investigated crop site. However, the small variation of R^2 between Sim_A and Sim_B also reveals that

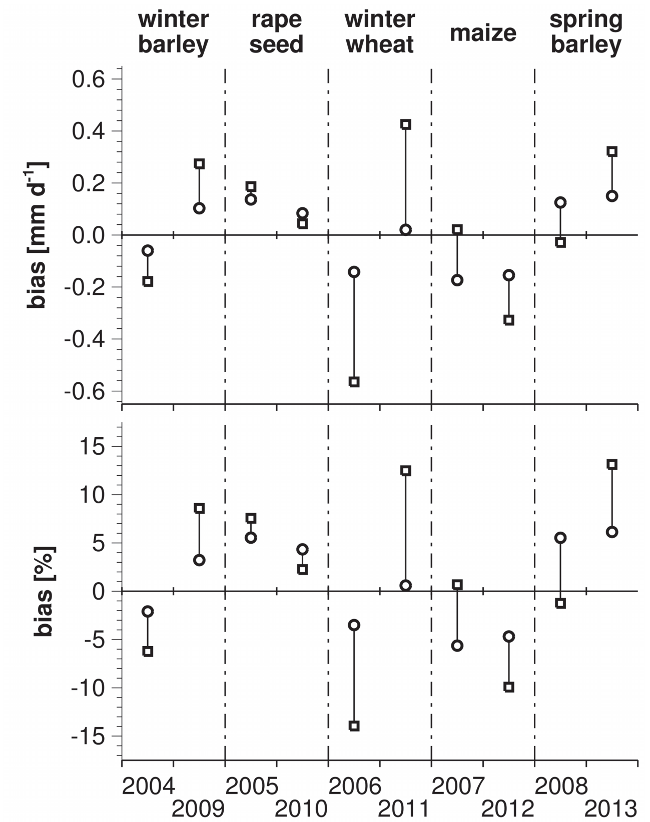

Figure 4: Bias in mm d^{-1} (upper plot) and in % (lower plot) for ET_{Mod} based on $g_{c,Ref}$ in relation to ET_{Ref}; open circles: $\mathrm{Sim_A}$, open rectangle: $\mathrm{Sim_B}$ (Associated pairs of $\mathrm{Sim_A}$ and $\mathrm{Sim_B}$ are connected by a vertical solid line.)

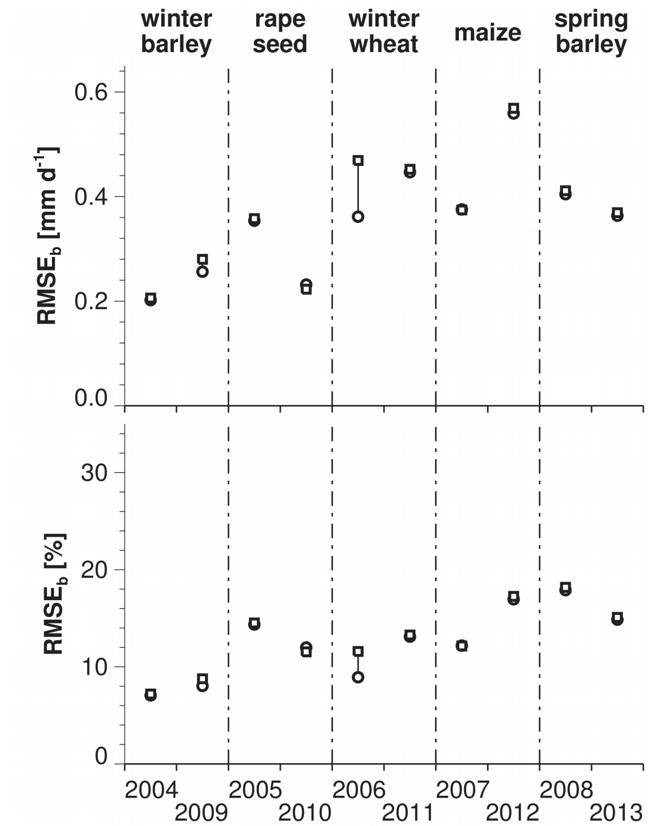

Figure 5: Bias corrected root mean square error ($RMSE_b$) in mm d^{-1} (upper plot) and in % (lower plot) for ET_{Mod} based on $g_{c,Ref}$ in relation to ET_{Ref}; open circles: $\mathrm{Sim_A}$, open rectangle: $\mathrm{Sim_B}$ (Associated pairs of $\mathrm{Sim_A}$ and $\mathrm{Sim_B}$ are connected by a vertical solid line.)

the correct simulation of general tendencies is largely independent from the parameterization of g_c.

In contrast to this, the quantitative correctness of ET_{Mod} is very sensitive to g_c which can be easily derived from Eq. (2.12). The bias of $\mathrm{Sim_A}$ varied between -0.17 mm d^{-1} (-5.6 %) and 0.15 mm d^{-1} (6.1 %). $RMSE_b$ of $\mathrm{Sim_A}$ was in range of 0.20 mm d^{-1} (7.0 %) and 0.56 mm d^{-1} (17.9 %). It should be noted that minima and maxima for bias and $RMSE_b$ occurred in different years. Furthermore, depending on whether the absolute value or the normalized value of $RMSE_b$ was considered the year in which the maximum value occurred changed. Based on typical characteristics of bias and $RMSE_b$, the magnitude of background uncertainty could be evaluated, i.e., the uncertainty of accuracy could be assessed to be ±5 %; for the uncertainty of precision, a magnitude of 15 % can be assumed. Therefore, the whole background uncertainty, being mainly caused by model and data imperfections (see Section 2.10.), is of the same magnitude as the uncertainty of measured ET which is encircled by ET_{EC} and ET_{EB}.

The bias of $\mathrm{Sim_B}$ was more than two times larger than the bias of $\mathrm{Sim_A}$ in most years. The observed minimum and maximum were -0.57 mm d^{-1} (-14.0 %) and 0.43 mm d^{-1} (13.1 %), respectively. Please note that maxima of absolute and normalized values occurred in different years which also holds for $RMSE_b$. Despite the general characteristic, the bias of $\mathrm{Sim_B}$ was lower than the bias of $\mathrm{Sim_A}$ in 2010, 2007 and 2008. This phenomenon can be easily explained. The estimates of $g_{c,\max}$ (and therefore of $g_{c,Ref}$) are based on the median to characterise the data sample of g_c within PHPA. Thus, the inserted vale of g_c is representative to characterize the data sample; however, it is not a calibrated value in terms of "a best fit". In contrast to the bias, $RMSE_b$ of $\mathrm{Sim_B}$ was very similar to $\mathrm{Sim_A}$. The related minimum and maximum were -0.21 mm d^{-1} (7.2 %) and 0.57 mm d^{-1} (18.2 %), respectively. Thus, it can be concluded that the parameterisation of g_c mainly affects the accuracy of simulation. However, its impact on its precision is negligible.

4 Summary and conclusions

The daily surface conductance (g_c) has been investigated for five different crops: winter barley, winter rape seed, winter wheat, silage maize, and spring barley. The investigations are based on EC measurements observing mass and energy exchange at field scale and are representative for the specific crop. Two complete cycles of crop rotation have been monitored. The special objective was the determination of representative maxima of

g_c ($g_{c,\max}$) which occur within the period of highest plant activity (PHPA).

A significant correlation between g_c and LUE was observed within the growing season. This correlation can be used as a proxy to evaluate the plant-physiological activity. With the help of this proxy, it was possible to define PHPA, and $g_{c,\max}$ could be determined. It was found that LUE is also a suitable indicator to separate periods, where ET is mainly caused by transpiration and periods, where soil evaporation is the major component of ET. In doing so, it could be assessed that g_c of a wet soil could take values as large as or even larger than g_c of vital plants. This suggests that a fallow field can evaporate high amounts of water and these periods should be considered in annual balances of ET accordingly.

The canopy height h_c was critically inspected whether it is a suitable proxy to evaluate plant-physiological activity. Results indicate that it is an improper variable for this. The relative curves of h_c and g_c do only agree at the beginning of the growing season. However, they significantly differ in the following phenological development stages. It should be noted that this disagreement occurs in the stages before the ripening stage already. Therefore, it is not an effect of the ripening stage. This result has highly practical relevance as h_c is often used in numerical water balance models to scale $g_{c,\max}$ with the underlying assumption that this parameterisation of g_c would be proper to simulate ET of a specific period. However, our results clearly demonstrate that this proceeding leads to an incorrect assessment of g_c and subsequently to shortcomings in simulated ET. A better solution might be the implementation of a scaling routine based on objective phenological characteristics, e.g., based on the BBCH classification (JKI, 2015).

g_c has been inversely computed from LE based on EC measurement data. The obtained values of g_c and especially $g_{c,\max}$ have been investigated for effects of measurement uncertainties. The energy balance closure gap (EBCG) was assessed as major source of uncertainty. The average EBCG was 19 % within PHPA but around 30 % for the whole period which are typical values. EBCG was used to address the potential range of LE's and ET's measurement uncertainty. In line with this, reference values of LE and ET (LE_{Ref} and ET_{Ref}, respectively) were obtained by partitioning EBCG via Bowen's ratio to the turbulent fluxes of H and LE. The effect of EBCG on estimates of g_c is enormous. In relation to g_c derived from LE_{Ref} (referred to as $g_{c,Ref}$), deviations of more than 50 % could be observed for determined values of $g_{c,\max}$ depending on the method which were utilized to address EBCG. This large uncertainty should be taken into account when estimates of g_c from different authors are compared and if it is not unequivocally stated whether and how EBCG were handled.

Based on $g_{c,Ref}$, crop specific estimates of $g_{c,\max}$ were determined for the first (and the second) cycle of crop rotation: winter barley, 19.2 mm s^{-1} (16.0 mm s^{-1}); winter rape seed, 12.3 mm s^{-1} (13.1 mm s^{-1}); winter wheat, 16.5 mm s^{-1} (11.2 mm s^{-1}); silage maize, 7.4 mm s^{-1} (8.5 mm s^{-1}); and spring barley, 7.0 mm s^{-1} (6.2 mm s^{-1}). Thus, a qualitative ranking of $g_{c,\max}$ was possible; from low to high: spring grain (spring barley and maize), rape seed, winter grain (winter wheat and winter barley). One can assume that the potential range of variation for crop specific g_c is not completely addressed in our study as effects of the genetic variation (e.g., Kelliher et al., 1995) or influences of water stress, nutrient availability and agricultural management (e.g., Schulze et al. 1994) could not be investigated. Although, we would like to stress that the utilized data set is significantly larger and more comprehensive than in most comparable studies. Thus, the presented values of $g_{c,\max}$ are still a reliable guideline for well water and nutrient supplied crop sites with similar climatic characteristics and similar soils.

Acknowledgements

This study was supported by the German Science Foundation (DFG) in the frame of the project "Model Based Classification of the Water Balance of Forest Sides in Low-range Mountain Areas" (FE 504/2-2) and "External factors of eco-technological water management – influences of land use and climate change" (BE 1721/13-1). The measurements at the test sites were supported by a series of EU projects including EUROFLUX (ENVCT 0095-0078), CARBOEUROFLUX (ENVK2-1999-00229) and CARBOEUROPE-IP (GOCE-CT-2003-505572), the BMBF project "VERTIKO" (#07ATF37-UBAS), and the TU Dresden. We acknowledge Uwe Eichelmann and Heiko Prasse for their technical assistance. Special thanks go to Mr. Tobias Fuchs, Dr. Valeri Goldberg, and the unknown reviewer for their pleasant support and useful comments. We also acknowledge the support by DFG, TU-Dresden and Saxon State and University Library Dresden (SLUB) for financing the Open Access Fees.

References

Asanuma, J., I. Tamagawa, H. Ishikawa, Y. Ma, T. Haysashi, Y. Qi, J. Wang, 2007: Spectral similarity between scalars at very low frequencies in the unstable atmospheric surface-layer over the Tibetan plateau. – Bound.-Layer Meteor. **122**, 85–103.

Aubinet, M., A. Grelle, A. Ibrom, Ü. Rannik, J. Moncrieff, T. Foken, A.S. Kowalski, P.H. Martin, P. Berbigier, C. Bernhofer, R. Clement, J. Elbers, A. Granier, T. Grünwald, K. Morgenstern, K. Pilegaard, C. Rebmann, W. Snijders, R. Valentini, T. Vesala, 1999: Estimates of the Annual Net Carbon and Water Exchange of Forests: The EUROFLUX Methodology. – Adv. Ecol. Res. **30**, 113–175.

Aubinet, M., T. Vesala, D. Papale, 2012: Eddy covariance: a practical guide to measurement and data analysis. – Springer, Dordrecht, New York, 438 pp.

Avissar, R., 1993: Observations of leaf stomatal conductance at the canopy scale: an atmospheric modelling perspective. – Bound.-Layer Meteor. **64**, 127–148.
Barr, A.G., K. Morgenstern, T.A. Black, J.H. McCaughey, Z. Nesic, 2006: Surface energy balance closure by the eddy-covariance method above three boreal forest stands and implications for the measurement of the CO2 flux. – Agric. For. Meteor. **140**, 322–337.
Bernhofer, C., 1993: Experimentelle Bestimmung von Energieflüssen über Pflanzenbeständen. – Habilitationsschrift in "Angewandter Meteorologie" an der Universität für Bodenkultur, Wien, 168 pp.
Bernhofer, C., J.H. Blanford, R. Siegwolf, M. Wedler, 1996: Applying single and two layer canopy models to derive conductances of a Scots pine plantation from micrometeorological measurements. – Theor. Appl. Climatol. **53**, 95–104.
Bernhofer, C., M. Aubinet, R. Clement, A. Grelle, T. Grünwald, A. Ibrom, P. Jarvis, C. Rebmann, E.D. Schulze, J.D. Tenhunen, 2003: Spruce forests (Norway and Sitka spruce, including Douglas fir): Carbon and water fluxes and balances, ecological and ecophysiological determinants. – In: Valentini, R. (Ed.): Fluxes of Carbon, Water and Energy of European Forests. – Ecological Studies **163**, Springer, 99-123.
Blanken, P.D., T.A. Black, P.C. Yang, H.H. Neumann, Z. Nesic, R. Staebler, G. den Hartog, M.D. Novak, X. Lee., 1997: Energy Balance and Canopy Conductance of a Boreal Aspen Forest: Partitioning Overstory and Understory Components. – J. Geophys. Res. Atmos. **102**, D24, DOI: 10.1029/97JD00193.
Breuer, L., H.-G. Frede, 2003: PlaPaDa - an online plant parameter data drill for eco-hydrological modelling approaches. – Published online: http://www.uni-giessen.de/~gh1461/plapada/plapada.html (accessed at 8.8.2015).
Burba, G., 2013: Eddy covariance method for scientific, industrial, agricultural, and regulatory applications: a field book on measuring ecosystem gas exchange and areal emission rates. – LI-COR Biosciences, 345 pp.
Charuchittipan, D., W. Babel, M. Mauder, J.P. Leps, T. Foken, 2014: Extension of the averaging time in eddy-covariance measurements and its effect on the energy balance closure. – Bound.-Layer Meteor. **152**, 303–327. DOI: 10.1007/s10546-014-9922-6.
Culf, A.D., T. Foken, J.H.C. Gash, 2004: The Energy Balance Closure Problem. – In: Kabat, P., M. Claussen, P.A. Dirmeyer, J.H.C. Gash, L.B. de Guenni, M. Meybeck, R.A.P. Sr, C.I. Vörösmarty, R.W.A. Hutjes, S. Lütkemeier (Eds.): Vegetation, Water, Humans and the Climate. – Springer, 159–166.
Eder, F., F. de Roo, K. Kohnert, R.L. Desjardins, H.P. Schmid, M. Mauder, 2014: Evaluation of two energy balance closure parametrizations. – Bound.-Layer Meteor. **151**, 195 – 219
Falge, E., D. Baldocchi, R. Olson, P. Anthoni, M. Aubinet, C. Bernhofer, G. Burba, R, Ceulemans, R. Clement, H. Dolman, A. Granier, P. Gross, T. Grünwald, D. Hollinger, N.-O. Jensen, G. Katul, P. Keronen, A. Kowalski, C.T. Lai, B.E. Law, T. Meyers, J. Moncrieff, E. Moors, J.W. Munger, K. Pilegaard, Ü. Rannik, C. Rebmann, A. Suyker, J. Tenhunen, K. Tu, S. Verma, T. Vesala, K. Wilson, S. Wofsy, 2001a: Gap filling strategies for long term energy flux data sets. – Agric. For. Meteor. **107**, 71–77.
Falge, E., D. Baldocchi, R. Olson, P. Anthoni, M. Aubinet, C. Bernhofer, G. Burba, R, Ceulemans, R. Clement, H. Dolman, A. Granier, P. Gross, T. Grünwald, D. Hollinger, N.-O. Jensen, G. Katul, P. Keronen, A. Kowalski, C.T. Lai, B.E. Law, T. Meyers, J. Moncrieff, E. Moors, J.W. Munger, K. Pilegaard, Ü. Rannik, C. Rebmann, A. Suyker, J. Tenhunen, K. Tu, S. Verma, T. Vesala, K. Wilson, S. Wofsy, 2001b: Gap filling strategies for defensible annual sums of net ecosystem exchange. – Agric. For. Meteor. **107**, 43–69.
Foken, T., 2008: Micrometeorology. – Springer, Berlin, Heidelberg, 308 pp.
Foken, T., B. Wichura, 1996: Tools for quality assessment of surface-based flux measurements. – Agric. Forest. Meteor. **78**, 83–105.
Foken, T., M. Aubinet, J.J. Finnigan, M.Y. Leclerc, M. Mauder, K.T. Paw U, 2011: Results of a Panel Discussion about the Energy Balance Closure Correction for Trace Gases. – Bull. Amer. Meteor. Soc. **92**, ES13–ES18.
Franssen, H.J.H., R. Stöckli, I. Lehner, E. Rotenberg, S.I. Seneviratne, 2010: Energy balance closure of eddy-covariance data: A multisite analysis for European FLUXNET stations. – Agric. Forest. Meteor. **150**, 1553–1567.
Grünwald, T., C. Bernhofer, 2007: A decade of carbon, water and energy flux measurements of an old spruce forest at the Anchor Station Tharandt. – Tellus B **59**, 387–396.
Halldin, S., A. Lindroth, 1992: Errors in net radiometry: comparison and evaluation of six radiometer designs. – J. Atmos Oceanic Technol. **9**, 762–783.
Ingwersen, J., K. Steffens, P. Högy, K. Warrach-Sagi, D. Zhunusbayeva, M. Poltoradnev, R. Gäbler, H.D. Wizemann, A. Fangmeier, V. Wulfmeyer, T. Streck, 2011: Comparison of Noah simulations with eddy covariance and soil water measurements at a winter wheat stand. – Agric. Forest. Meteor. **151**, 345–355.
JKI (Julius Kühn-Institute): BBCH scale. – Published online: http://www.jki.bund.de/de/startseite/veroeffentlichungen/bbch-codes.html (21.6. 2015).
Kelliher, F.M., R. Leuning, M.R. Raupach, E.D. Schulze, 1995: Maximum conductances for evaporation from global vegetation types. – Agric. Forest. Meteor, **73**, 1–16.
Klemeš, V., 1983: Conceptualization and scale in hydrology. – J. Hydrol. **65**, 1–23.
Kljun, N., P. Calanca, M. Rotach, H. Schmid, 2004: A Simple Parameterisation for Flux Footprint Predictions. – Bound.-Layer Meteor. **112**, 503–523.
Kohsiek, W., C. Liebethal, T. Foken, R. Vogt, S.P. Oncley, C. Bernhofer, H.A.R. de Bruin, 2007: The energy balance experiment EBEX-2000. Part III: behavior and quality of radiation measurements. – Bound.-Layer Meteor. **123**, 55–75.
Körner, C., 1995: Leaf diffusive conductances in the major vegetation types of the globe. – In: Schulze, E.D., M.M. Caldwell (Eds.): Ecophysiology of Photosynthesis. Ecological Studies **100**, Springer, 463–490.
Leclerc, M.Y., T. Foken, 2014: Footprints in Micrometeorology and Ecology. – Springer, 239pp.
Leuning, R., J. Moncrieff, 1990: Eddy-covariance CO2 flux measurements using open- and closed-path CO_2 analysers: Corrections for analyser water vapour sensitivity and damping of fluctuations in air sampling tubes. – Bound.-Layer Meteor. **53**, 63–76.
Leuning, R., E. van Gorsel, W.J. Massman, P.R. Isaac, 2012: Reflections on the surface energy imbalance problem. – Agric. Forest. Meteor. **156**, 65–74.
Lindroth, A., M. Mölder, F. Lagergren, 2010: Heat storage in forest biomass improves energy balance closure. – Biogeoscience **7**, 301–313.
Mauder, M., T. Foken, 2006: Impact of post-field data processing on eddy covariance flux estimates and energy balance closure. – Meteorol. Z. **15**, 597–609

Mauder, M., S.P. Oncley, R. Vogt, T. Weidinger, L. Ribeiro, C. Bernhofer, T. Foken, W. Kohsiek, H.A.R. de Bruin, H. Liu, 2007: The energy balance experiment EBEX-2000. Part II: Intercomparison of eddy-covariance sensors and post-field data processing methods. – Bound.-Layer Meteor. **123**, 29–54.

Mauder, M., M. Cuntz, C. Drüe, A. Graf, C. Rebmann, H.P. Schmid, M. Schmidt, R. Steinbrecher, 2013: A strategy for quality and uncertainty assessment of long-term eddy-covariance measurements. – Agric. For. Meteor. **169**, 122–135.

McMahon, T.A., M.C. Peel, L. Lowe, R. Srikanthan, T.R. McVicar, 2013. Estimating actual, potential, reference crop and pan evaporation using standard meteorological data: a pragmatic synthesis. – Hydrol. Earth Syst. Sci. **17**, 1331–1363.

Moderow, U., C. Bernhofer, 2014: Cluster of the Technische Universität Dresden for greenhouse gas and water fluxes. – ILEAPS-Newsletter, Special issue on environmental research infrastructures, 34 – 37.

Moderow, U., M. Aubinet, C. Feigenwinter, O. Kolle, A. Lindroth, M. Mölder, L. Montagnani, C. Rebmann, C. Bernhofer, 2009: Available energy and energy balance closure at four coniferous forest sites across Europe. – Theor. Appl. Climatol. **98**, 397–412.

Moffat, A.M., D. Papale, M. Reichstein, D.Y. Hollinger, A.D. Richardson, A.G. Barr, C. Beckstein, B.H. Braswell, G. Churkina, A.R. Desai, E. Falge, J.H. Gove, M. Heimann, D. Hui, A.J. Jarvis, J. Kattge, A. Noormets, V.J. Stauch, 2007: Comprehensive comparison of gap-filling techniques for eddy covariance net carbon fluxes. – Agric. Forest. Meteor. **147**, 209–232.

Moncrieff, J.B., Y. Malhi, R. Leuning, 1996: The propagation of errors in long-term measurements of land-atmosphere fluxes of carbon and water. – Global Change Biology **2**, 231–240.

Monteith, J.L., 1965: Evaporation and Environment. The State and Movement of Water in Living Organisms. – Symposium of the Society of Experimental Biology **19**, Cambridge University Press, 205–234.

Monteith, J.L., 1990: Principles of environmental physics, Second edition. – Butterworth Heinemann, 291 pp.

Moore, C.J., 1986: Frequency response corrections for eddy correlation systems. – Bound.-Layer Meteor. **37**, 17–35.

Oncley, S.P., T. Foken, R. Vogt, W. Kohsiek, H.A.R. de Bruin, C. Bernhofer, A. Christen, E. van Gorsel, D. Grantz, C. Feigenwinter, I. Lehner, C. Liebethal, H. Liu, M. Mauder, A. Pitacco, L. Ribeiro, T. Weidinger, 2007: The Energy Balance Experiment EBEX-2000. Part I: overview and energy balance. – Bound.-Layer Meteor. **123**, 1–28.

Panin, G.N., C. Bernhofer, 2008: Parametrization of turbulent fluxes over inhomogeneous landscapes. – Izv. Atmos. Ocean. Phys. **44**, 701–716.

Penman, H., 1948: Natural Evaporation from Open Water, Bare Soil and Grass. – Proc. R. Soc. Lond. Ser. Math. Phys. Sci. **193**, 120–145.

Prescher, A.-K., T. Grünwald, C. Bernhofer, 2010: Land use regulates carbon budgets in eastern Germany: From NEE to NBP. – Agric. Forest. Meteor. **150**, 1016–1025.

Rannik, Ü., A. Sogachev, T. Foken, M. Göckede, N. Kljun, M.Y. Leclerc, T. Vesala, 2012: Footprint Analysis. – In: Aubinet, M., T. Vesala, D. Papale (Eds.): Eddy Covariance. – Springer Netherlands, 211–261.

Reichstein, M., E. Falge, D. Baldocchi, D. Papale, M. Aubinet, P. Berbigier, C. Bernhofer, N. Buchmann, T. Gilmanov, A. Granier, T. Grünwald, K. Havrankova, I. lvesniemi, D. Janous, A. Knohl, T. Laurila, A. Lohila, D. Loustau, G. Matteucci, T. Meyers, F. Miglietta, J.-M. Ourcival, J. Pumpanen, S. Rambal, E. Rotenberg, M. Sanz, J. Tenhunen, G. Seufert, F. Vaccari, T. Vesala, D. Yakir, R. Valentini, 2005: On the separation of net ecosystem exchange into assimilation and ecosystem respiration: review and improved algorithm. – Glob. Change Biol. **11**, 1424–1439.

Richter, F., C. Döring, M. Jansen, O. Panferov, U. Spank, C. Bernhofer, 2015: How to Predict Hydrological Effects of Local Land Use Change: How the Vegetation Parameterisation for Short Rotation Coppices Influences Model Results. – Hydrol. Earth Syst. Sci., **19**, 3457–3474. DOI:10.5194/hess-19-3457-2015.

Ruppert, J., M. Mauder, C. Thomas, J. Lüers, 2006: Innovative gap-filling strategy for annual sums of CO_2 net ecosystem exchange. Agric. Forest. Meteor., **138**, 5–18.

Schotanus, P., F.T.M. Nieuwstadt, H.A.R. de Bruin, 1983: Temperature measurement with a sonic anemometer and its application to heat and moisture fluxes. – Bound.-Layer Meteor. **26**, 81–93.

Schulze, E.-D., F.M. Kelliher, C. Körner, J. Lloyd, R. Leuning, 1994: Relationships Among Maximum Stomatal Conductance, Ecosystem Surface Conductance, Carbon Assimilation Rate, and Plant Nitrogen Nutrition: A Global Ecology Scaling Exercise. – Ann. Rev. Ecol. Systematics **25**, 629–60.

Shuttleworth, W.J., 2012. Canopy Processes and Canopy Resitances. – In: Shuttleworth, W.J. (Ed.): Terrestrial hydrometeorology, 301–315.

Shuttleworth, W.J., J.S. Wallace, 1985: Evaporation from sparse crops – An energy combination theory. – Quart. J. Roy. Meteor. Soc. **111**, 839–855.

Spank, U., 2010: Site Water Budget: Influences of Measurement Uncertainties on Measurement Results and Model Results. – Published online: http://nbn-resolving.de/urn:nbn:de:bsz:14-qucosa-62557 (10.12.2010).

Spank, U., C. Bernhofer, 2008: Another simple method of spectral correction to obtain robust eddy-covariance results. – Bound.-Layer Meteor. **128**, 403–422.

Spank, U., K. Schwärzel, M. Renner, U. Moderow, C. Bernhofer, 2013: Effects of measurement uncertainties of meteorological data on estimates of site water balance components. – J. Hydrol. **492**, 176–189.

Sposito, G., 2008: Scale dependence and scale invariance in hydrology. – Cambridge University Press, 444 pp.

Stannard, D.I., 1993: Comparison of Penman-Monteith, Shuttleworth-Wallace, and modified Priestley-Taylor evapotranspiration models for wildland vegetation in semiarid rangeland. – Water Resour. Res. **92**, 1379–1392.

Stoy, P.C., G.G. Katul, M.B.S. Siqueira, J.Y. Juang, K.A. Novick, H.R. McCarthy, A.C. Oishi, J.M. Uebelherr, H.S. Kim, R.A.M. Oren, 2006: Separating the effects of climate and vegetation on evapotranspiration along a successional chronosequence in the southeastern US. – Global Change Biol. **12**, 2115–2135.

Stoy, P.C., M. Mauder, T. Foken, B. Marcolla, E. Boegh, A. Ibrom, M.A. Arain, A, Arneth, M. Aurela, C. Bernhofer, A. Cescatti, E. Dellwik, P. Duce, D. Gianelle, E. van Gorsel, G. Kiely, A. Knohl, H. Margolis, H. McCaughey, L. Merbold, L. Montagnani, D. Papale., M. Reichstien, M. Saunders, P. Serraon-Ortiz, M. Sottocornola, D. Spano, F. Vaccari, A. Varlagein, 2013: A data-driven analysis of energy balance closure across FLUXNET research sites: The role of landscape scale heterogeneity. – Argic. Forest. Meteor. **171–172**, 137–152.

Tchiguirinskaia, I., M. Bonell, P. Hubert, 2004: Scales in hydrology and water management. – IAHS press, 170 pp.

The University of Edinburgh School of GeoSciences, Institute of Atmospheric and Environmental Science, 2007: EdiRe. – Published online: http://www.geos.ed.ac.uk/abs/research/micromet/EdiRe/ (accessed at 8.8.2015)

Twine, T.E., W.P. Kustas, J.M. Norman, D.R. Cook, P.R. Houser, T.P. Meyers, J.H. Prueger, P.J. Starks, M.L. Wesely, 2000: Correcting eddy-covariance flux underestimates over a grassland. – Agric. Forest. Meteor. **103**, 279–300.

Vicente-Serrano, S.M., J.I. López-Moreno, 2005: Hydrological response to different time scales of climatological drought: an evaluation of the Standardized Precipitation Index in a mountainous Mediterranean basin. – Hydrol. Earth Syst. Sci. Discuss. **9**, 523–533.

Vickers, D., L. Mahrt, 1997: Quality Control and Flux Sampling Problems for Tower and Aircraft Data. – J. Atmos. Ocean. Technol. **14**, 512–26.

Vogt, R., C. Bernhofer, L.W. Gay, L. Jaeger, E. Parlow, 1996: The available energy over a Scots Pine plantation. What's up for partitioning? – Theor. Appl. Climatol. **53**, 23–31.

Wang, K., R.E. Dickinson, 2012: A review of global terrestrial evapotranspiration: Observation, modeling, climatology, and climatic variability. – Rev. Geophys. **50**, RG2005, DOI: 10.1029/2011RG000373.

Wilczak, J.M., S.P. Oncley, S.A. Stage, 2001: Sonic Anemometer Tilt Correction Algorithms. – Bound.-Layer Meteor. **99**, 127–150.

Wilson, K., A. Goldstein, E. Falge, M. Aubinet, D. Baldocchi, P. Berbigier, C. Bernhofer, R. Ceulemans, H. Dolman, C. Field, A. Grelle, A. Ibrom, B.E. Law, A. Kowalski, T. Meyers, J. Moncrieff, R. Monson, W. Oechel, J. Tenhunen, R. Valentini, S. Verma, 2002a: Energy balance closure at FLUXNET sites. – Agric. Forest. Meteor. **113**, 223–243.

Wilson, K.B., D.D. Baldocchi, M. Aubinet, P. Berbigier, C. Bernhofer, H. Dolman, E. Falge, C. Field, A. Goldstein, A. Granier, A. Grelle, T. Halldor, D. Hollinger, G. Katul, B.E. Law, A. Lindroth, T. Meyers, J. Moncrieff, R. Monson, W. Oechel, J. Tenhunen, R. Valentini, S. Verma, T. Vesala, S. Wofsy, 2002b: Energy Partitioning between Latent and Sensible Heat Flux during the Warm Season at Fluxnet Sites: Energy Balance Partitioning at Fluxnet Sites. – Water Resour. Res. **38**, 30-1–30-11. DOI: 10.1029/2001WR000989.

Wohlfahrt, G., C. Irschick B. Thalinger, L. Hörtnagl, N. Obojes, A. Hammerle, 2010: Insights form independent evapotranspiration estimates for closing the energy balance: A grassland case study. – V. Zone **9**, 1025-1033.

Xu, C.-Y., V.P. Singh, 1998: A Review on Monthly Water Balance Models for Water Resources Investigations. – Water Res. Manag. **12**, 20–50.